Development of a Susceptor-Free Induction Welding System for Continuous Joining of Carbon Fiber Thermoplastic Composites

A. Cai, S. Salemi, and M. Tehrani*
[1] Department of Structural Engineering, University of California San Diego, La Jolla, CA, USA
*tehrani@ucsd.edu

Keywords: *Induction Welding; Thermoplastic Composites; Carbon Fiber/PEEK; System Development; Closed-Loop Temperature Control*

1. Abstract

Thermoplastic composites (TPCs) are increasingly used in aerospace structures owing to their capacity for fusion bonding during assembly and repair. While some welding techniques rely on an embedded metallic susceptor that remains permanently at the bond interface, susceptor-free approaches such as induction heating generate heat directly at the joint by leveraging the electrical conductivity of the reinforcement fibers themselves, albeit with a risk of localized overheating from edge effects and contact-resistance current concentration that necessitates temperature management. This work presents the design, manufacture, and development of a susceptor-free induction welding platform for joining carbon fiber/polyether-ether-ketone (CF/PEEK) laminates, organized into three phases: first, a benchtop induction welding system incorporating a closed-loop feedback control system integrated with a thermal imaging camera to establish reliable temperature management across varied sample materials and geometries; second, the extension of this capability to continuous welding through a static welding station equipped with stepper motor-driven linear translation of the workpiece, enabling the production of continuous lap-shear weld coupons under controlled traverse speed and vacuum bag compaction; and third, the conceptual design and initial prototyping of a compact welding end-effector intended for robotic arm integration, combining a pressure roller with the induction heating work head to facilitate automated continuous welding operations, with experimental validation of the robotic end-effector left as a direction for future investigation. The system is designed with the objective of enabling low-temperature bonding strategies, such as the use of amorphous polyetherimide (PEI) interlayers at the bond interface, which permit joining at temperatures below the melt temperature of the semi-crystalline PEEK matrix, and the present contribution focuses on the instrumentation, control architecture, and mechanical design of the welding platform itself, establishing the foundation upon which subsequent processing studies will be conducted.

2. Introduction

Thermoplastic composites (TPCs) have emerged as a material of significant interest in aerospace applications owing to their inherent advantages over thermoset alternatives, including higher toughness, recyclability, and the capacity for fusion bonding (colloquially referred to as ‘welding’) [1]. Unlike thermoset based composites which require mechanical fastening or adhesive bonding for joining, TPCs can be remelted and fused at the bond interface, creating a structural joint that results in a single, homogenous composite part with no discernible joint surface [2]. This characteristic is particularly attractive in automated manufacturing processes, where welding techniques can be directly integrated into the assembly process, leading to significant time and cost savings. To meet the throughput demands of automated aerospace assembly, high processing speeds are of significant industrial interest; however, the rapid and transient thermal cycles inherent to fast welding processes introduce additional complexities with respect to the processing of the polymer matrix.

2.1. Carbon Fiber/PEEK Composite Joining

Among the high performance TPC material systems of interest to the aerospace industry, one of the most prominent is carbon fiber reinforced polyether-ether-ketone (CF/PEEK), a high performance semi-crystalline thermoplastic which offers excellent mechanical properties, high chemical resistance, and low thermal expansion [3]. PEEK presents three coupled challenges for welding. Firstly, its high melting temperature (~343 °C) requires precise interfacial temperature control to drive interdiffusion without thermal degradation [4]. Furthermore, semi-crystalline morphology (30–35% crystallinity in CF/PEEK [5]) is locally erased and reformed during welding, with the recovered crystallinity governed by cooling rate [6]. Lastly, at fast traverse speeds, sharp increases in viscosity from cooling limits polymer percolation into surface asperities [7]. Collectively, these challenges motivate the need for welding systems that can deliver precise and repeatable thermal profiles at the bond interface.

2.2. Induction Welding of Thermoplastic Composites

Welding techniques for thermoplastic composites can be classified by their heat generation mechanism into thermal (e.g., hot plate, infrared laser), friction (e.g., ultrasonic, vibration), and electromagnetic methods. Thermal methods require a changeover phase that risks oxidation and degradation [1], while friction-based techniques can disturb local fiber orientation [1]. Electromagnetic methods such as resistance and induction welding generate heat in situ while the adherends remain stationary under sustained compaction. Resistance welding, the most established electromagnetic technique, embeds a conductive susceptor at the bond interface and supplies current through contacting electrodes, which introduces a foreign material, creates sensitivity to current leakage under high compaction, and constitutes a contact heating method [1, 8].

In contrast, induction heating is a contactless electromagnetic method for heat generation. An alternating current in a conducive coil, typically copper, produces an alternating magnetic field that induces eddy currents in a nearby conductive workpiece, which dissipates as heat via Joule losses [9, 10]. The efficacy of heating is governed by coil geometry, standoff distance, and workpiece properties such as electrical conductivity, magnetic permeability, and geometry. Coil geometry can be designed to accommodate flat panels, single- and double-curved surfaces, and hollow cylindrical tubes [11, 12], with flexibility in coil design limited only by materials and manufacturability. The introduction of additive manufacturing techniques such as fused filament fabrication and laser powder bed fusion has enabled complex geometries that were previously infeasible through conventional bending and brazing [13, 14].

For fiber-reinforced composites, the reinforcing fiber itself must be electrically conductive and contain a closed-loop pathway to allow eddy current generation directly in the laminate, with the induced currents dissipating energy according to Joule's law [9]. Three principal heat generation mechanisms have been identified in induction heating of carbon fiber reinforced composites: Joule loss in fibers, dielectric hysteresis heating at ply junctions, and contact resistance heating at fiber-fiber junctions [10]. Joule losses, otherwise referred to as fiber heating, arise from the electrical resistance of the carbon fibers and depend on fiber length, resistivity, and cross-sectional area [15]. Dielectric hysteresis heating occurs at interfaces where fibers in adjacent plies are separated by thin layers of polymer matrix, where the alternating electric field results in a capacitor-like effect and generates heat through molecular charge movement within the polymer [16]. Contact resistance heating occurs when fiber-to-fiber contact is high, producing temperature- and pressure-dependent resistance at fiber junctions [17]. Recent literature suggests that susceptor-less induction welding is dominated primarily by Joule heating of fibers — in laminates with plies of different fiber orientations, the magnitude of heat generation was found to be greatest along the fiber direction, with polymer or dielectric heating observed only when the entire laminate consisted of layers all oriented in the same direction [18].

3. System Design and Development

The induction heating hardware forms the core of the welding system. Power is delivered to the induction workhead by an Ambrell EasyHeat 8310LI solid-state induction power supply rated at 10 kW, paired with an Ambrell EasyHeat LI 3542 workhead. Cooling for the induction coil and workhead is provided by a JHI-2000M liquid chiller (Dimplex Thermal Solutions) rated at 24,000 BTU/hr cooling capacity, supplying water at a flow rate of 10 GPM through a closed-loop refrigeration circuit. The induction coil used throughout all characterization and development experiments is a single-turn hairpin coil manufactured by Ambrell, representative of coil geometries commonly employed in aerospace induction welding applications. The coil geometry and dimensions are depicted in Figure X.

The workhead is mounted to an aluminum frame equipped with linear sliders and a leadscrew adjustment mechanism coupled to a digital readout, enabling precise control of the coil standoff distance from 0 to 150 mm with a resolution of 0.25 mm. Springs are incorporated to offset the weight of the workhead and reduce the load transmitted to the leadscrew mechanism. A vortex tube chiller supplies cold air directed to the top surface of the workpiece, mitigating surface overheating that can occur due to the concentration of eddy currents near the coil-facing surface as described by the skin effect. Compaction is achieved through vacuum bagging, delivering up to 0.1 MPa of uniform pressure across the weld zone. This approach is well-suited for benchtop characterization of lap shear specimens, as it accommodates a range of sample geometries without requiring dedicated fixtures or retooling between configurations.

The operating frequency is determined by the circuit formed by the capacitors within the workhead and the impedance of the coil-workpiece system. As the coil current increases, the load on the circuit increases and results in a drop in frequency. For the present coil geometry and carbon fiber composite workpieces, coil currents between 400 and 600 A yield an operating frequency range of 275 to 375 kHz, consistent with frequency ranges reported in the literature for susceptor-free induction heating of carbon fiber reinforced thermoplastics [10, 12]. The interdependence of current and frequency means that the primary user-controlled parameter is the coil current (and by extension the power output), while the frequency is a dependent variable governed by the system's electrical characteristics. As the relationship between penetration depth and volumetric heat generation is highly dependent on the specific material system and coil configuration, empirical characterization of the system's thermal response becomes necessary to achieve consistent weld parameters.

3.1. Phase 1: Thermal Camera Feedback Control/Benchtop Characterization

The first step in developing the induction welding cell was to establish reliable closed-loop temperature control at the bond interface. This was accomplished through the integration of real-time thermal imaging with automated power supply control. A FLIR A700 infrared thermal camera provides continuous surface temperature measurements, which are acquired through a custom C++ program interfacing directly with the camera's API. The program processes the incoming temperature data and issues commands to the EasyHeat power supply over RS485 serial connection, adjusting the output current and dwell time of the alternating current in real time. This enables the implementation of a PID control loop that regulates heat generation in the laminate based on the measured top surface temperature. Under static heating conditions, the PID controller maintained the setpoint temperature within ±0.5 °C indefinitely, with tunable parameters yielding a time-to-temperature of 1.5 s to 300 °C. The level of thermal control demonstrated is sufficient to maintain the narrow processing window between the glass transition of PEI and the melt temperature of PEEK.

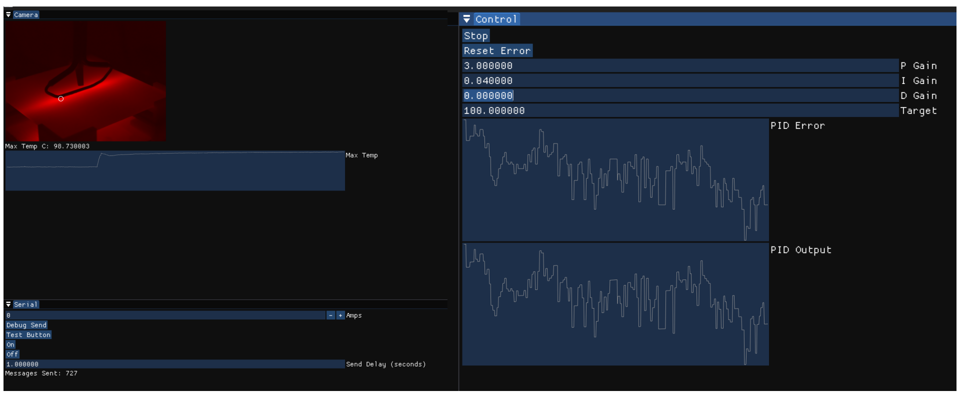

Figure 1. PID control interface with integrated FLIR thermal camera monitoring

However, the FLIR A700 captures only the exposed top surface temperature and does not have direct line of sight to the bond interface during a weld operation. To address this, the through-thickness temperature gradient was characterized empirically by using a picture frame fixture in conjunction with embedded thermocouples at the bottom surface of the laminate, opposite the coil. Separate calibration experiments were conducted at matched power settings, in which the top surface temperature recorded by the thermal camera was correlated with simultaneous bottom surface thermocouple readings across a range of laminate configurations and processing conditions. The resulting calibration relationships enable the closed-loop controller to infer the bond interface temperature from the top surface measurement alone and regulate it accordingly. While the present implementation relies on FLIR thermal camera feedback, the PID controller is equally compatible with thermocouple input, providing a direct measurement of the joint interface temperature in scenarios where the camera's line of sight to the laminate surface is blocked, such as when a heat sink is applied to manage surface overheating.

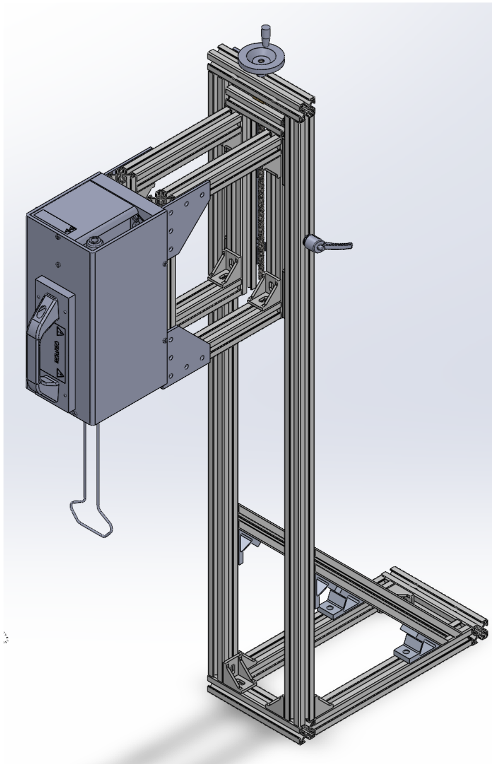

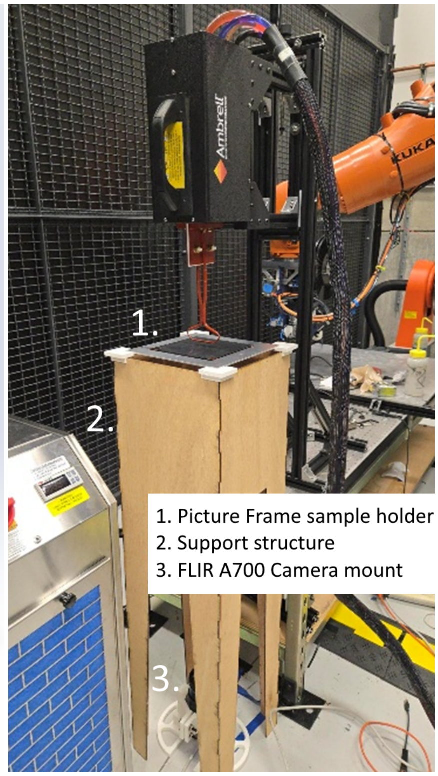

(a). *(b).*

Figure 2. (a) CAD model of the workhead support structure, and (b) picture frame fixture and support structure for characterizing the temperature distribution.

Characterization experiments were conducted on 16 ply carbon fiber/PEEK cross-ply laminates with a $[0/90]_{4s}$ stacking sequence, fabricated from Toray TC1200/T700GC unidirectional tape using a vacuum bag-only process (VBO) consolidation process. VBO was selected as the method of fabrication owing to its capacity to produce laminates with low void content, ensuring sufficient fiber-to-fiber contact for eddy current generation [17, 19]. Because VBO consolidation pressures are lower than those achieved in autoclave or hot press processing, a long VBO cycle was employed to maximize the degree of interply fiber-to-fiber contact in the laminates used for induction welding characterization [19]

3.2. *Phase 2: Linear Motion Continuous Welding*

With closed-loop thermal control established, development progressed toward the manufacture of lap shear specimens. Per ASTM D5868-01, lap shear specimens require an overlap region of 25.4 x 25.4 mm. However, characterization of the hairpin coil's thermal footprint during picture frame experiments revealed a heat zone of approximately 5 x 60 mm, spanning the full width of the overlap but covering only a fraction of its length in the weld direction. To produce a fully consolidated weld across the entire overlap region, continuous welding capability is required, resulting in the development of a linear translation mechanism to move the heating zone along the length of the weld line.

Linear translation of the workpiece is driven by a stepper motor controlled through an Arduino microcontroller, with provisions for zeroing, homing, programmable start and stop positions, and adjustable traverse speeds ranging from 0.1 to 20 mm/s. The translation stage features interchangeable configurations that allow workpiece motion in two orientations -

parallel or perpendicular to the length of the induction coil, with a total travel range of 195 mm in either direction. The two orientations allow for different heat patterns as the thermal zone sweeps across the overlap and are shown in Figure 4.

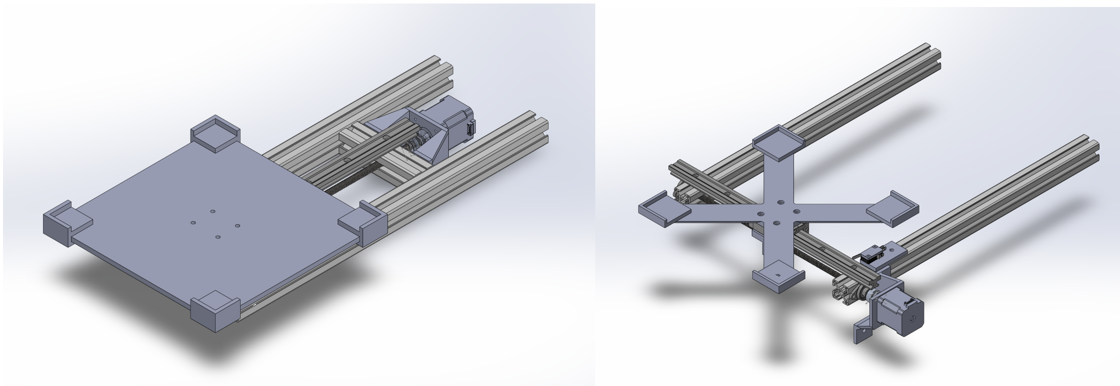

(a). *(b).*

Figure 3. Linear slider mechanisms for perpendicular (a) and parallel (b) motion

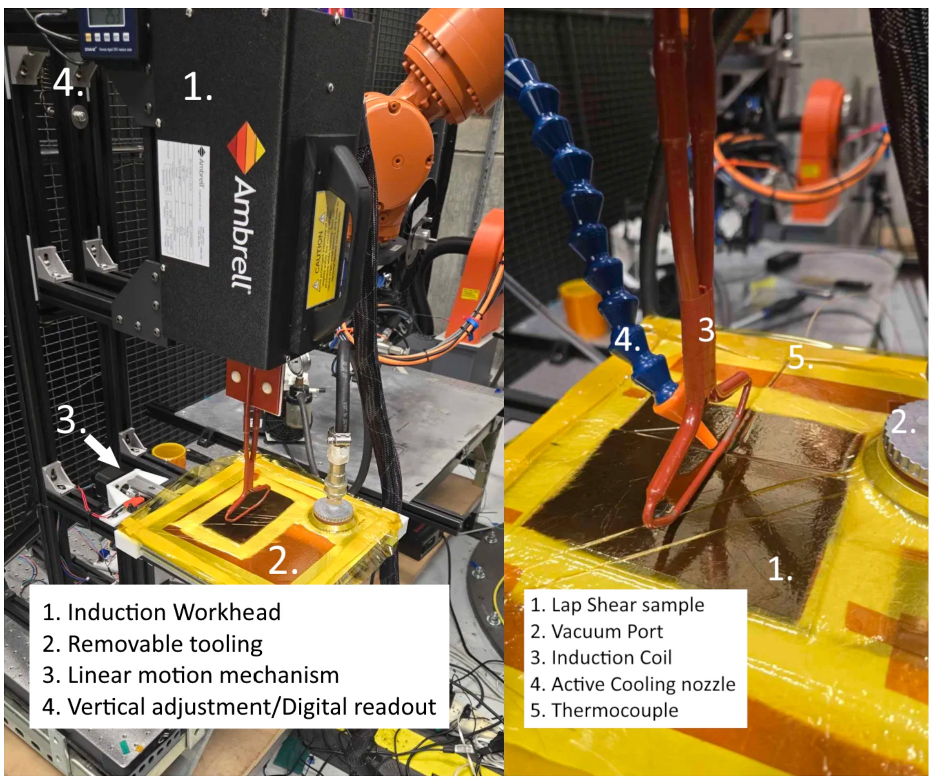

Figure 4. Induction welding system with surface cooling

3.3. Phase 3: Modular End-Effector Design/Robotic Manufacturing Cell Integration

In parallel with the development of the static welding station and linear translation system, a compact welding end-effector was designed and prototyped for integration with a KUKA KR 160 R1570 Nano 6-axis industrial robot. The KUKA robot arm is part of an existing automated fiber placement (AFP) cell used for the manufacture of thermoplastic composite laminates. The compact induction welding end effector was designed as part of a broader initiative to establish a comprehensive thermoplastic processing and manufacturing cell within this infrastructure. Modularity and interchangeability were central design considerations, as the end effector features a mounting interface compatible with the existing AFP head, enabling rapid tool changes between manufacturing operations. This allows sequential processing workflows in which laminates can be first manufactured in-situ using the AFP head and subsequently joined using the induction welding end-effector on the same robotic platform.

In contrast to the vacuum bag compaction used in Phases 1 and 2, the end-effector employs an integrated pressure roller that is pneumatically actuated, enabling adjustable compaction pressure at the bond interface during continuous welding. The roller is sized for a 25.4 mm weld path, with the roller material and diameter selected to match those used in the existing AFP cell to maintain compatibility. The offset distance between the center of the heating zone and the roller nip point is adjustable, enabling the dwell time between heating and compaction to be tuned for a given set of processing parameters and traverse speeds. Shorter offset distances reduce the time for heated material to cool before consolidation, allowing for higher bond interface temperature at the point of compaction. Conversely, a longer offset allows for greater cooling prior to compaction, which may be desirable for managing residual stresses or controlling crystallinity development in the weld zone. The ability to vary this offset provides an additional degree of freedom in optimizing the continuous welding process.

Experimental validation of the robotic welding end-effector, including weld quality assessment and processing parameter optimization, lies beyond the scope of the present work and is proposed as a direction for future investigation.

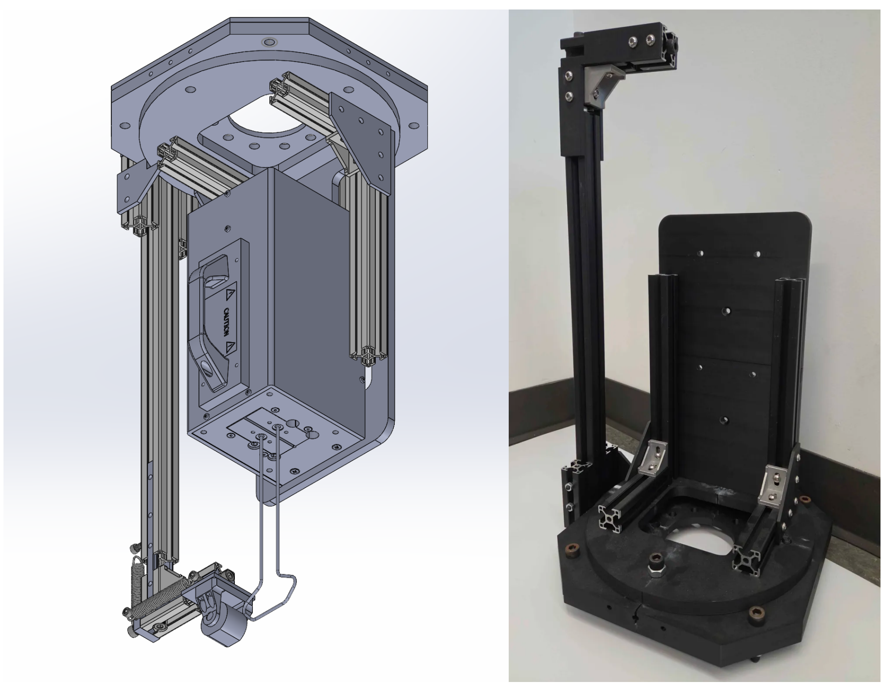

Figure 5. CAD model and 3D printed prototype of the compact end effector

4. Lap Shear Sample Fabrication

To validate the capabilities of the induction welding system developed in Phases 1 and 2, lap-shear specimens were manufactured and tested in accordance with ASTM D5868-01. The adherend laminates were fabricated using the same material system and processing techniques as the characterization samples: 16-ply CF/PEEK cross-ply laminates with a $[0/90]_{4s}$ stacking sequence, consolidated from Toray TC1200/T700GC unidirectional tape via a long VBO cycle. A 10-mil layer of neat PEI film was co-consolidated with the CF/PEEK laminate during the VBO cycle, forming a PEI-rich surface on the bonding face of each adherend. This amorphous interlayer enables fusion bonding at temperatures above the glass transition temperature of PEI but below the melting temperature of the PEEK matrix.

Lap-shear specimens were prepared by cutting the consolidated laminate (152.4 × 152.4 mm) in half and welding the two halves together with a 25.4 mm overlap in accordance with ASTM D5868-01. The exact setup of the lap shear sample is depicted in Figure X. Welding was performed at a coil current of 550 A and traverse speed of 0.5 mm/s, with the coil positioned 0.5 mm above the top surface of the laminate. These parameters produced a bond interface temperature of approximately 300°C, as inferred from the calibrated top surface-to-interface temperature offset established during Phase 1 characterization.

Samples of 25.4 mm width were then cut from the welded laminates and subject to tensile testing using a MTS 810 machine equipped with a 100 kN load cell, with a crosshead displacement rate of 13 mm/min. SLS strength was calculated using the equation:

$$\tau = \frac{F_{max}}{A_{overlap}} \quad \text{(Eq. 1)}$$

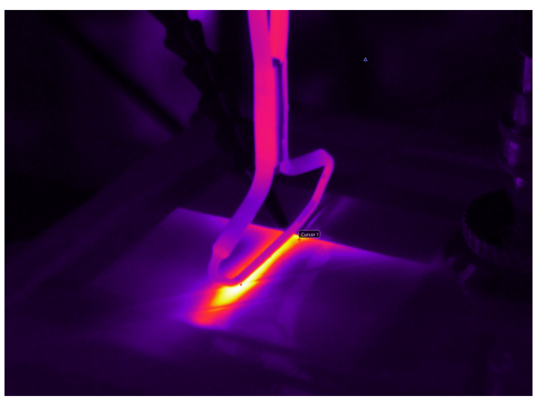

Figure 6. Thermal image of the weld zone during continuous induction welding.

5. Results and Discussions

5.1. Lap Shear Strength

Mechanical performance of the welded joints was evaluated via single-lap shear testing on an MTS universal testing machine. Across all specimens, an average lap shear strength of 31.4 ± 5.3 MPa across 4 samples were measured. This result falls within the range of values reported in the literature for susceptor-free induction welded CF/PEEK joints, both with and without a PEI interlayer at the bond interface (Table X).

Table 1. Comparison of lap shear strength values for induction welded CF/PEEK joints

Reference	LSS (MPa)	Sample Thickness	Laminate type	Weld configuration	Welding method
Present work	31.4± 5.3	2.35 mm	Carbon/PEEK	Co-consolidated PEI interlayer	Induction
Border and Salas (1989)	27	16 ply (~2 mm)	Carbon/PEEK	No insert	Induction
Cogswell et al. (1989)	31	1.5 – 2 mm	Carbon/PEEK	No insert	Induction
Schwartz (1994)	38–48	NR	Carbon/PEEK	No insert	Induction
Cogswell et al. (1989)	36	NR	Carbon/PEEK	PEEK film insert	Induction
Border and Salas (1989)	44	NR	Carbon/PEEK	PEEK film insert	Induction
Todd et al. (1990)	33	NR	Carbon/PEEK	PEI/PEEK film	Induction
Smiley et al. (1989)	49	16 ply (~2mm)	Carbon/PEEK	PEI interlayer (Thermabond)	Resistance
Korycki et al. (2022)	17.6	1 mm	Carbon/PEEK	No insert	Induction
Dupuis et al. (2022)	15.2	NR	PEI on CF/PEEK	PEI substrate	Laser

6. Conclusions

This work presented the design, manufacture, and development of a susceptor-free induction welding platform for joining carbon fiber/PEEK laminates, organized across three progressive phases. Preliminary validation was performed using single-lap shear specimens fabricated from 16-ply $[0/90]_{4s}$ CF/PEEK laminates with a co-consolidated PEI interlayer, welded at a coil current of 550 A and a traverse speed of 0.5 mm/s. The use of an amorphous PEI interlayer at the bond interface enables joining above the glass transition of PEI while remaining below the melt temperature of the semi-crystalline PEEK matrix, thereby preserving the crystalline microstructure and mechanical integrity of the parent laminate. The resulting joints exhibited an average lap shear strength of 31.4 ± 5.3 MPa, consistent with values reported in the literature for susceptor-free induction-welded CF/PEEK joints and confirming the platform's capacity to produce structurally meaningful welds without melting the PEEK matrix. The instrumentation, control architecture, and mechanical design established here provide the foundation for subsequent processing studies, including experimental validation of the robotic end-effector and systematic optimization of weld parameters.

7. Acknowledgements

This work was supported by the Office of Naval Research (ONR) grant #N00014-24-1-2178.

References

[1] Yousefpour, A., Hojjati, M., & Immarigeon, J.P. (2004). Fusion Bonding/Welding of Thermoplastic Composites. Journal of Thermoplastic Composite Materials, 17(4), 303–342.

[2] R.P. Wool, B.-L. Yuan and O.J. McGarel, "Welding of polymer interfaces," Polymer Science and Engineering, vol. 29, no. 19, pp. 1340–1367, 1989.

[3] Gabrion, X., Placet, V., Trivaudey, F., & Boubakar, L. (2016). About the thermomechanical behaviour of a carbon fibre reinforced high-temperature thermoplastic composite. Composites Part B: Engineering, 95, 386–394.

[4] Levy, A., Helaili, S., & Gillespie, J.W. (2009). Computational and experimental analysis of fusion bonding in thermoplastic composites: Influence of process parameters. Journal of Materials Processing Technology, 209(9).

[5] Nara, S. et al. (2003). The crystallinity of PEEK composites. Composites Science and Technology.

[6] Lee, W.I., Talbott, M.F., Springer, G.S., & Berglund, L.A. (1987). Effects of Cooling Rate on the Crystallinity and Mechanical Properties of Thermoplastic Composites. Journal of Reinforced Plastics and Composites, 6, 2–12.

[7] Kirchhoff, J., Ghattas, O., & Tehrani, M. (2024). Resin percolation and intimate contact in fast processing of thermoplastic composites. Composites Part A, 182, 108145.

[8] Stavrov, D. & Bersee, H.E.N. (2005). Resistance welding of thermoplastic composites — an overview. Composites Part A: Applied Science and Manufacturing, 36, 39–54.

[9] Haimbaugh, R.E. (2001). Practical Induction Heat Treating. ASM International.

[10] Ahmed, T.J., Stavrov, D., Bersee, H.E.N., & Beukers, A. (2006). Induction welding of thermoplastic composites — an overview. Composites: Part A, 37, 1638–1651.

[11] Cano, R.J., Grimsley, B.W., Czabaj, M.W., & Hull, B.Z. (2023). Consolidation of Braided Carbon Fiber/Thermoplastic Tubes by Induction Heating. NASA Technical Reports Server, NASA/TM-2023-0008687.

[12] Barazanchy, D. (2022). The effect of induction welding coil shape on heat generation. AIAA SciTech 2022 Forum, San Diego, CA, January 3–7, 2022. AIAA 2022-0406.

[13] Schüßler, P., Franke, J., Czink, S., Antusch, S., Mayer, D., Laube, S., Hanemann, T., Schulze, V., & Dietrich, S. (2023). Characterization of the Metal Fused Filament Fabrication Process for Manufacturing of Pure Copper Inductors. Materials, 16(20), 6678.

[14] Martin, J.D. (2017). Exploring Additive Manufacturing Processes for Direct 3D Printing of Copper Induction Coils. Proceedings of the ASME 2017 International Mechanical Engineering Congress and Exposition, Volume 2: Advanced Manufacturing, Tampa, FL, November 3–9, 2017, V002T02A026. ASME.

[15] Mitschang, P., Rudolf, R., & Neitzel, M. (2002). Continuous induction welding process, modelling and realisation. Journal of Thermoplastic Composite Materials, 15, 127–153.

[16] Fink, B.K., McCullough, R.L., & Gillespie Jr, J.W. (1992). A local theory of heating in cross-ply carbon fiber thermoplastic composites by magnetic induction. Polymer Engineering and Science, 32(5), 357–369.

[17] Yarlagadda, S., Kim, H.J., Gillespie Jr, J.W., Shevchenko, N.B., & Fink, B.K. (2002). A study on the induction heating of conductive fiber reinforced composites. Journal of Composite Materials, 36(4), 401–421.

[18] Barazanchy, D. (2023). Heating mechanisms in induction welding of thermoplastic composites. Journal of Thermoplastic Composite Materials.

[19] Khaleghi, S., Kirchhoff, J.G., Pandher, J., Lacalle, J., & Tehrani, M. (2026). Efficient consolidation of thermoplastic composites using AFP-engineered air channels and optimized VBO processing. *Composites Part B*, 310, 113134.